

## Reactive transport of trace elements and isotopes in the Eutaw coastal plain aquifer, Alabama

Ming-Kuo Lee,<sup>1</sup> James Griffin,<sup>1</sup> James Saunders,<sup>1</sup> Yang Wang,<sup>2</sup> and Jiin-Shuh Jean<sup>3</sup>

Received 1 June 2006; revised 13 October 2006; accepted 12 February 2007; published 30 May 2007.

[1] We integrate groundwater geochemistry, mineralogy, and numerical modeling techniques to study the reactive transport of heavy metals and isotopes in the Eutaw coastal plain aquifer, Alabama. Geochemical data show that the elevated concentrations of Fe, Mn, and Sr can be correlated with high pH and alkalinity. These geochemical correlations suggest that that elevated metal concentrations may be derived from bacterial iron and manganese reduction. Geochemical modeling of bacterial Fe(III) and Mn(IV) reduction shows that the biotransformation of iron and manganese minerals could control mobility and concentrations of Fe and Mn in coastal plain aquifers. Petrographic, SEM, and EDAX studies of sediments show the formation of biogenic siderite, rhodochrosite, and pyrite in sediments associated with Fe- and Mn-rich groundwater. Rhodochrosite and siderite occur together as spheroids ( $\approx 1.0$  mm) in which rhodochrosite forms the center and siderite forms an outer rind, which is consistent with the redox sequence of mineral precipitation predicted by the geochemical modeling. The low  $\delta^{13}\text{C}$  ratios of siderite and rhodochrosite ( $-14.4$  to  $-15.4\%$ , PDB) and groundwater DIC ( $-20.6$  to  $-14.1\%$ , PDB) imply carbon of biogenic origin. Higher DIC- $\delta^{13}\text{C}$  levels are found to be correlated with elevated Fe and Mn concentrations and high pH values of groundwater. This unexpected result implies novel carbon isotopic fractionation processes associated with bacterial Fe(III) reduction. We used  $^{36}\text{Cl}/\text{Cl}$  ratios of groundwater and isotope transport modeling to calculate the residence time of regional groundwater in the Eutaw aquifer. The calculation considering the natural decay only would yield  $^{36}\text{Cl}$  levels that are significantly higher than field data, suggesting that a significant mixing with Cl-rich, older groundwater at depth is an important reason for substantial  $^{36}\text{Cl}$  depletion along flow path.

**Citation:** Lee, M.-K., J. Griffin, J. Saunders, Y. Wang, and J.-S. Jean (2007), Reactive transport of trace elements and isotopes in the Eutaw coastal plain aquifer, Alabama, *J. Geophys. Res.*, 112, G02026, doi:10.1029/2006JG000238.

### 1. Introduction

[2] Water chemistry of the regional coastal plain aquifer systems has raised much concern in recent years because the aquifers have been exploited for large quantities of drinking water. Studies by *Back and Hanshaw* [1970], *Lee* [1985, 1993], and *Penny et al.* [2003] gave important insight to geochemical evolution of groundwater on the basis of regional geochemical data and mineral saturation states. *Chapelle and Knobel* [1983] and *Appelo* [1994] have investigated the inorganic ion exchange between aquifer sediments and recharging fresh groundwater. A number of geochemists have used stable isotopes to assess groundwa-

ter sources [e.g., *Clark and Fritz*, 1997] and biomineralization processes [*Zhang et al.*, 2001; *Romanek et al.*, 2003], as well as radioactive tracers to estimate groundwater recharge rates [e.g., *Bentley et al.*, 1986; *Lehmann et al.*, 1993; *Johnson et al.*, 2000; *Roback et al.*, 2001; *Alley et al.*, 2002; *Carey et al.*, 2004]. Microbial activities have been investigated and documented in coastal plain aquifers of South Carolina and Alabama [*Murphy et al.*, 1992; *Lovley et al.*, 1990; *Lovley and Chapelle*, 1995; *Chapelle*, 2001; *Penny et al.*, 2003; *Park et al.*, 2006] where various microorganisms are responsible for iron, manganese, and sulfate reduction reactions that significantly modify groundwater geochemistry. Because the possible biogeochemical reactions in regional aquifers are quite complex, hydrologists have used numerical modeling techniques to study hydrological transport processes and the nature of water-sediment-bacteria interaction [e.g., *Plummer et al.*, 1990; *Bethke*, 1989; *Lee and Saunders*, 2003; *Lee et al.*, 2005]. To date, however, little has been done to quantify or model reactive transport processes in coastal plain aquifers.

[3] For over 150 years the Eutaw aquifer has been an important resource for central-south Alabama, and continues

<sup>1</sup>Department of Geology and Geography, Auburn University, Auburn, Alabama, USA.

<sup>2</sup>Department of Geological Sciences, Florida State University, Tallahassee, Florida, USA.

<sup>3</sup>Department of Earth Sciences, National Cheng Kung University, Tainan, Taiwan.

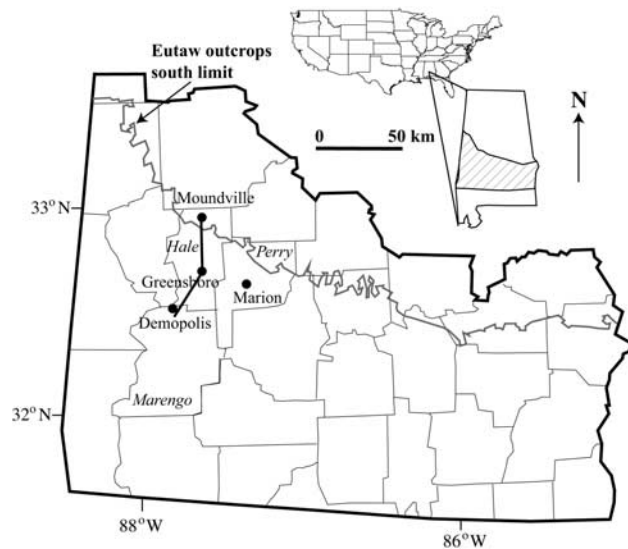


**Figure 1.** Location map of the investigated area in central-west Alabama. Also shown are the southern limit of the recharge outcrop of the Eutaw aquifer (thin grey line) and cities in Hale, Perry, and Marengo counties where groundwaters were sampled (see Table 1 for well locations). Hydrostratigraphy was reconstructed along the Hale-Marengo transect (bold line) in groundwater flow and isotope transport modeling.

today supplying water for more than 250,000 residents in 18 counties [Cook, 1993]. There have been many studies concerning the geology, stratigraphy, hydrology, and geochemistry of aquifers in central Alabama [Lee, 1985; King, 1990; Planert *et al.*, 1993; Barker and Pernik, 1994; Floesser, 1996; Cook, 1993, 1997]. Despite its importance as a major source of water supply, the origin of trace metals, the nature of water-sediment-bacteria interaction, freshwater recharge rates, and the influence of microbial processes on water chemistry remain poorly understood. Field data indicate that high metal concentrations correlate with elevated alkalinity levels and pH values in groundwater [Penny *et al.*, 2003]. Fe(III)-reducing bacteria, found in the Fe- and Mn-rich groundwaters in western Alabama [Penny *et al.*, 2003], could utilize organic matter deposited in sediments to grow and reduce Fe(III) and Mn(IV) oxides; this bacterial reduction process would release aqueous  $\text{Fe}^{2+}$ ,  $\text{Mn}^{2+}$ , and other trace metals such as  $\text{Sr}^{2+}$  and  $\text{Ba}^{2+}$  that have been adsorbed or coprecipitated by oxides. The sequential peaks of  $\text{Ca}^{2+}$ ,  $\text{Mg}^{2+}$ ,  $\text{K}^{+}$ , and  $\text{Na}^{+}$  along the flow paths indicate that separation of ions may be driven by ion exchange between groundwater and sediments like glauconite, which are abundant in the Eutaw Formation [Cook, 1993; Davis, 1998]. We hypothesize that groundwater geochemistry in the Alabama coastal plain aquifers is strongly influenced by (1) bacterial Fe(III)- and Mn(IV)-reduction; (2) inorganic ion exchange and calcite dissolution; (3) hydrolysis of silicate minerals; (4) biomineralization of carbonate and pyrite minerals; and (5) physical mixing of different types of groundwater. In this paper, the term biomineralization is defined loosely as any biologically induced or controlled mineralization since actual biogeochemical

processes by which bacteria directly form or precipitate minerals remain poorly understood and are difficult to prove. We investigate how the chemical composition of Eutaw groundwater evolves by various geochemical and microbial processes as it moves deeper into the subsurface. The main objectives include (1) determining the sources of elevated metals, alkalinity, and reactive carbon in the Eutaw aquifer; (2) characterizing the biomineralization processes in Fe- and Mn-rich groundwater and their effects on bulk water chemistry; (3) modeling  $^{36}\text{Cl}$  transport and assessing recharge rates in the Eutaw aquifer; and (4) developing a reactive transport model of solutes and isotopes in the Eutaw coastal plain aquifer of Alabama.

## 2. Geology and Hydrogeology

[4] The Cretaceous strata of the coastal plain physiographic province in central Alabama consist of a thick wedge of marine sediments that crop out in a discrete band stretching approximately 360 km across the central portion of the state. The sediments unconformably overlie the crystalline Paleozoic basement of the Piedmont [Horton *et al.*, 1984; King, 1990]. The sediments of the lower strata (Coker, Gordo, and Eutaw Formations) are typically poorly indurated and composed of sand, gravel, and silt. The upper strata (Selma Group) consist of well indurated sediments such as chalk, limestone, and sandstone.

[5] This study focuses on the hydrology and geochemistry of the shallow portion of the Eutaw Formation situated in the west-central Alabama coastal plain. Groundwater sampling sites are located in the cities of Moundville, Marion, Greensboro, and Demopolis in Hale, Perry, and Marengo counties (Figure 1). The study area stretches approximately 50 km from the recharge/outcrop area and trends southwest toward the Gulf of Mexico. This portion of the Eutaw Formation is subject to significant recharge and contains fresh water resources that are important for public water supplies and also used for agricultural needs such as catfish production, livestock production, and irrigation. The Eutaw Formation outcrop is approximately 32 km wide in western Alabama and narrows extensively eastward to less than 8 km in eastern Alabama. The Eutaw Formation dips variably from southwestward in the west part of Alabama, to south in the eastern portion of the state, with a gradient typically less than 1% [Cook, 1993].

[6] The Eutaw Formation consists of light to green-gray, cross-laminated, fine to medium, well-sorted, micaceous, glauconitic sand [Raymond and Copeland, 1987; King, 1990]. The Eutaw Formation is distinctly coarser and contains more marine glauconitic materials than the Tuscaloosa Formation [King, 1990]. A clay zone separates the Eutaw Formation into the upper well-cemented sandstone and lower clay interbedded with sand. The upper confining units of the Eutaw aquifer, the Mooreville Chalk, Demopolis Chalk, and Blufftown Formation are low-permeability, micaceous and calcareous clays. The lower confining unit, the upper part of the Gordo Formation, is mostly clay.

[7] Groundwater recharges along east-west and northwest-southeast outcrop trends in central Alabama (Figure 1). Groundwater migrates generally to the south in central-east Alabama, and moves southwest in the western part of the study area, following the dip of the aquifers. Groundwater is

pumped from the sandy portion of the aquifers throughout the study area. In some locations, the continuous sand portion of the coastal plain aquifers yields up to 1 million gallons (3780 m<sup>3</sup>) of water per day [Cook, 1993].

### 3. Methods

#### 3.1. Groundwater Sampling and Geochemical Analysis

[8] Geochemical and isotope analyses have been conducted on groundwater samples taken along a transect southward from recharge areas in western Alabama (Figure 1). The transect follows regional flow lines beginning in the updip portion of the study area near Moundville, and continues downdip into Demopolis. Prior to collection, wells were purged an average of 15 min to remove groundwater inside well casings from periods of inactive pumping. After purging, raw water was collected in a plastic beaker, in which temperature, pH, Eh, and specific conductance were directly measured using hand-held instruments. During the measurements, the beaker was covered with lid in order to reduce the atmospheric exposure and measured errors. Data acquisition began when the reading became stable. A raw and an acidified sample from each well and their replicates were sent to ACTLABS for major ion and trace element analysis using inductively coupled plasma mass spectrometry (ICP-MS). The ICP-MS is capable of quantitatively determining concentrations of trace elements in liquids in the range of fractions of a part per billion. The precision of ICP-MS analysis is generally 1~3% for heavy metals. Samples for trace element and cation analyses were passed through a 0.45  $\mu\text{m}$  filter, acidified with concentrated HNO<sub>3</sub>, and stored in polyethylene bottles. Water bottles were leached by 3% HNO<sub>3</sub> before sampling to ensure trace metal cleanliness. Anion concentrations were measured in the laboratory using a Dionex 2000 ion chromatograph (IC). All samples were filtered prior to analysis using a 0.2  $\mu\text{m}$  nylon filter. The  $\delta^{13}\text{C}$  analysis of dissolved inorganic carbon (DIC) in groundwater was performed by the Isotope Geochemistry Section of the Illinois State Geological Survey.

#### 3.2. Well-Cutting Analysis

[9] Well-cutting samples were taken from screened intervals of Fe-rich groundwater wells in the study area, including Moundville, Marion, Greensboro, and Demopolis. Samples were obtained from the well core storage facility at the Geological Survey of Alabama in Tuscaloosa, Alabama. Well cuttings consisted mainly of unconsolidated coastal plain sediments that were collected and boxed at the time of well construction. Samples were analyzed using X-ray diffraction to determine bulk mineralogy. Sediments grains exhibiting secondary mineral overgrowths in Fe- and Mn-rich zones were analyzed by a field emission scanning electron microscope (SEM) and an energy dispersive X-ray spectroscope (EDS). Energy dispersive spectroscopy analysis is performed in conjunction with the SEM for identifying and quantifying elemental compositions of authigenic minerals including siderite (FeCO<sub>3</sub>) and rhodochrosite (MnCO<sub>3</sub>). Carbon isotopic ratios (<sup>13</sup>C) of authigenic siderite and rhodochrosite from the Marion and Demopolis wells were measured using the Finnigan MAT delta PLUS XP Mass Spectrometer at Florida State University.

#### 3.3. Numerical Reaction Path Modeling

[10] Modeling bacterial Fe(III)- and Mn(IV)-reduction along the flow path of the Eutaw aquifer was accomplished by using a numerical program Geochemist's Workbench (GWB) [Bethke, 1996; Lee and Bethke, 1996]. The initial conditions of the model were set according to the geochemical data of Moundville groundwater (MV1) upstream of the iron-reduction zone. The model first equilibrates to the Moundville groundwater at 25° C and assumes that the initial concentrations of Fe and Mn reflect equilibrium with hematite (Fe<sub>2</sub>O<sub>3</sub>) and pyrolusite (MnO<sub>2</sub>) in aquifers under aerobic conditions. The simulation then linearly reduces redox potential (Eh) from 700 mV to -200 mV and simultaneously titrates 500  $\mu\text{mol}$  of organic material (acetate) into 1 kg of fluid in the initial system. By lowering the Eh of the system and adding organic material, the model can simulate those mineralogical and geochemical reactions under which bacterial Fe(III)- and Mn(IV)-reduction occur. The model provides insights on groundwater geochemical evolution and the sequence of mineral reactions during the reductive dissolution of Fe- and Mn-oxides.

#### 3.4. Modeling Regional Flow, <sup>36</sup>Cl Transport, and Groundwater Residence Time

[11] The basin hydrology model Basin2 [Bethke et al., 1993] was used to simulate regional fluid flow and groundwater residence time by tracking the transport and natural decay of <sup>36</sup>Cl through the Eutaw aquifer. Basin2 uses a finite difference grid consisting of nodal blocks arranged into columns and rows that cover the entire two-dimensional basin cross-sectional area. To simulate groundwater flow, we first reconstructed a cross section that represents the stratigraphy and lithology of the coastal plain sediments in the study area. Thickness and composition of four different strata (i.e., the lower Tuscaloosa, the upper Tuscaloosa, the Eutaw Formation, and the Selma Group) in the cross section were synthesized from existing stratigraphic data [e.g., King, 1990; Raymond and Copeland, 1987; Davis, 1998; Cook, 1993]. On the basis of lithologic compositions of strata (see geology and hydrogeology section), a percentage of each end-member (sand and clay) component was estimated that closely represented the hydraulic properties of each unit [Bethke et al., 1993].

[12] We used Basin2 to quantify groundwater residence time as a function of calculated <sup>36</sup>Cl/Cl ratios. The radioactive isotope <sup>36</sup>Cl is naturally produced in the atmosphere by the bombardment of <sup>40</sup>Ar by cosmic rays [Bentley et al., 1986; Davis et al., 2000]. All samples analyzed in this study have less than approximately 2 tritium units (TU), indicating that groundwater contains negligible anthropogenic <sup>36</sup>Cl from nuclear explosions after 1952 [Penny et al., 2003]. After formation in the atmosphere, <sup>36</sup>Cl is dissolved into rainwater and subsequently infiltrates into the subsurface where the isotope is isolated from its atmospheric source and begins to slowly decay. Owing to its slow radioactive decay rate (half-life  $\approx$  301,000 years), <sup>36</sup>Cl can be used to date older groundwater that has migrated and resided in regional aquifers for millions of years. The residence time of groundwater can be calculated as

$$t = \frac{-1}{\lambda_{36}} \ln \frac{N_{36}}{N_{36}^0}, \quad (1)$$

**Table 1.** Municipal Wells Sampled With Locations by County and Latitude and Longitude Coordinates<sup>a</sup>

Sample Identification	Well Name	County	Location, Latitude/Longitude	Distance From Recharge, km
MV1	Moundville 1	Hale	32.57.18/87.37.10	0
MV2	Moundville 2	Hale	32.57.12/87.36.27	2
MCH	Marion-Chicken House	Perry	32.38.09/87.20.25	15
MHT	Marion-Hill Top	Perry	32.37.41/87.20.43	17
MMMI	Marion-MMI	Perry	32.37.55/87.20.02	18
GBCH	Greensboro-Court House	Hale	32.57.12/87.36.28	20
GBWS	Greensboro-Walton Street	Hale	32.42.15/87.35.33	21
GBSS	Greensboro-South Street	Hale	32.42.15/87.35.42	22
GBBG	Greensboro-Big	Hale	32.45.16/87.36.04	23
DEM1	Demopolis 1	Marengo	32.31.21/87.50.12	47
DEM2	Demopolis 2	Marengo	32.30.13/87.49.26	48
DEM3	Demopolis 3	Marengo	32.30.09/87.48.42	49
DEM5	Demopolis 5	Marengo	32.28.52/87.47.11	50

<sup>a</sup>Also included are distances of wells from the nearest aquifer recharge/outcrop area.

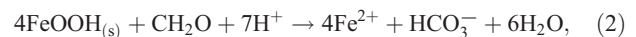
where  $N_{36}$  is the number of  $^{36}\text{Cl}$  atoms in a volume of groundwater and  $\lambda_{36}$  is the isotope's decay constant ( $\lambda = \ln 2/T_{1/2}$ , where  $T_{1/2}$  is half-life). We use a value for  $\lambda_{36}$  of  $2.31 \times 10^{-6} \text{ yr}^{-1}$  to calculate the rate at which  $^{36}\text{Cl}$  decays. Modeling results were integrated with  $^{36}\text{Cl}$  data collected in our previous study [Penny *et al.*, 2003] to interpret residence time and fresh water recharge rates. Because both natural decay of  $^{36}\text{Cl}$  with travel time and progressive mixing with old, deeper groundwater may be responsible for the decrease of  $^{36}\text{Cl}$  observed along the flow path, a comparison of modeling results (assuming natural decay only) with field data can provide insight on the extent of groundwater mixing and offer a check on the correctness of  $^{36}\text{Cl}/\text{Cl}$  in groundwater dating. Significant mixing with old groundwater would result in low  $^{36}\text{Cl}/\text{Cl}$  ratios and overestimation of groundwater ages.

## 4. Results and Discussion

### 4.1. Major Ion and Trace Element Geochemistry

[13] Concentrations or trends of major and trace elements from thirteen municipal wells (Tables 1 and 2) collected in this study and by Penny *et al.* [2003] were used to assess the geochemical processes and water-sediment-bacteria interaction in the Eutaw Formation. Along the flow transect, significantly higher alkalinity and pH in the Marion and Demopolis wells (Table 2) correspond to parallel increases in Fe, Mn, and Sr concentrations (Figure 2). These corre-

lations suggest that elevated Fe, Mn, and Sr concentrations may be derived from bacterial iron and manganese reduction similar to that proposed by Saunders *et al.* [1997, 2005] and Zobrist *et al.* [2000],



where  $\text{CH}_2\text{O}$  represents organic matter. Eh values of Fe-rich groundwaters in Marion and Demopolis range from  $-20$  to  $-100$  mV (Table 2); such moderately reducing conditions are favorable for bacterial iron reduction [Barcelona *et al.*, 1989]. The dissimilatory iron reduction would release metals and raise alkalinity of groundwater at the expense of  $\text{H}^+$ , organic carbon, and iron oxides. Concentrations of Sr also correlate well with dissolved Fe in the Ganges-Brahmaputra floodplain in the Bengal basin [Dowling *et al.*, 2003; Turner, 2006]. Recent experimental studies indicated that Sr can be sorbed to  $\text{FeOOH}$  solids and bacteria cell surfaces under oxidized conditions [e.g., Small *et al.*, 1999]. The sorbed Sr is subsequently mobilized when the redox conditions become favorable for bacterial iron reduction [Roden *et al.*, 2002; Dowling *et al.*, 2003]. Interestingly, other trace metals (Cu, Zn, Ba) generally parallel those trends found in Fe, Mn, and Sr with sequential rise and fall in concentrations (Table 2).

[14] Downgradient from the recharge area, a sequence of  $\text{Ca}^{2+}$ ,  $\text{Mg}^{2+}$ ,  $\text{K}^+$ , and  $\text{Na}^+$  dominated water along the flow path (Figure 3) indicates that ion exchange could control the

**Table 2.** Chemical and Isotopic Compositions of Selected Ions of Eutaw Groundwaters<sup>a</sup>

Sample Identification	Ca, mM	K, mM	Mg, mM	Na, mM	Cl, mM	SO <sub>4</sub> , mM	Fe, $\mu\text{M}$	Mn, $\mu\text{M}$	Sr, $\mu\text{M}$	Ba, $\mu\text{M}$	Zn, $\mu\text{M}$	Cu, $\mu\text{M}$	$\delta^{13}\text{C}$ , ‰	$^{36}\text{Cl}/\text{Cl} \times 10^{-15}$	pH	Eh, volts	Alkalinity, mM
MV1	0.04	0.06	0.04	0.06	0.05	0.02	0.04	0.03	0.46	0.44	0.36	0.03	-19.43	122	7.23	0.053	0.10
MV2	0.05	0.05	0.02	0.05	0.04	0.02	0.02	0.06	0.11	0.22	0.16	0.02	-19.29	...	7.22	0.051	0.13
MCH	0.32	0.07	0.17	0.09	0.08	0.04	157.56	7.50	5.12	1.02	0.35	0.03	-17.73	...	7.98	-0.027	0.43
MHT	0.39	0.08	0.21	0.09	0.07	0.02	171.89	8.34	6.07	1.18	0.23	0.0	-15.52	...	8.14	-0.020	0.53
MMMI <sup>b</sup>	0.68	0.12	0.30	0.13	0.06	0.08	6.20	0.49	5.14	1.48	0.09	0.05	...	105	7.02	-0.025	0.78
GBCH	0.06	0.12	0.05	0.07	0.06	0.11	3.53	0.16	0.78	0.44	0.45	0.16	-18.67	95	7.53	0.040	0.15
GBWS	0.05	0.10	0.05	0.06	0.07	0.03	1.00	0.06	0.76	0.40	2.74	2.13	-20.57	...	7.23	0.080	0.15
GBSS	0.05	0.10	0.05	0.06	0.06	0.03	0.25	0.02	0.72	0.36	0.44	0.10	-20.19	...	7.43	0.076	0.13
GBBG <sup>b</sup>	0.04	0.12	0.05	0.07	0.05	0.04	0.02	0.01	0.25	0.37	0.04	0.08	...	91	5.63	0.055	0.09
DEM1 <sup>b</sup>	0.03	0.02	0.02	9.26	3.00	<0.002	6.05	0.16	1.35	0.07	0.12	0.01	...	6	8.72	-0.018	2.79
DEM2	0.05	0.08	0.02	11.22	3.90	<0.002	0.25	0.10	1.52	0.01	0.05	0.05	-14.10	...	8.69	-0.101	3.70
DEM3	0.03	0.06	0.01	7.76	1.88	<0.002	0.39	0.10	0.82	0.01	0.05	0.04	-14.45	...	8.81	-0.105	3.05
DEM5 <sup>b</sup>	0.03	0.04	0.02	8.74	2.95	<0.002	8.56	0.14	1.11	0.06	1.62	0.01	...	8	8.66	-0.090	2.65

<sup>a</sup>Sample locations and well names are shown in Table 1. The  $^{36}\text{Cl}$  data are from Penny *et al.* [2003].

<sup>b</sup>Data from Penny *et al.* [2003].

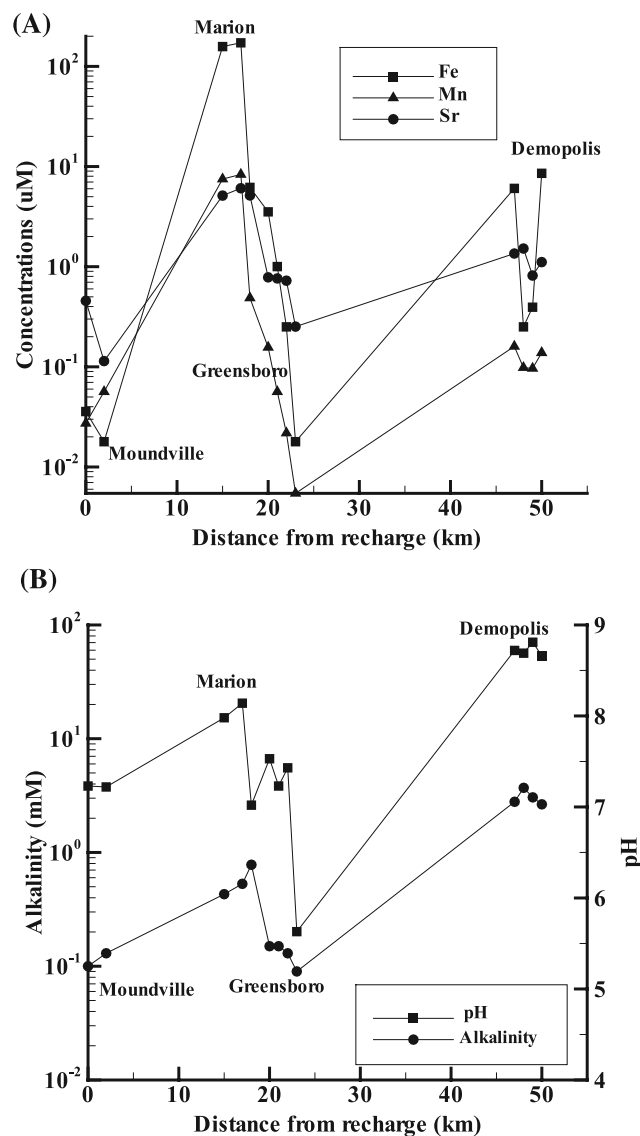
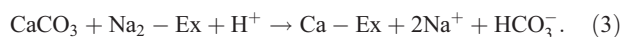


**Figure 2.** (a) Fe, Mn, and Sr concentrations (Table 2) of groundwater samples at various distances from recharge along the transect (Figure 1) in western Alabama. (b) Alkalinity and pH (Table 2) along the same transect.

bulk water chemistry. Ion exchange and concurrent calcite dissolution may also lead to the increasing pH and alkalinity of groundwater, much like bacterial Fe- and Mn-reduction, but they mainly release cations ( $\text{Ca}^{2+}$ ,  $\text{Mg}^{2+}$ ,  $\text{Na}^+$ ,  $\text{K}^+$ ) into solution. Calcite is common in Alabama coastal plain sediments and it is usually present as fossil shells and perhaps as cements [Lee, 1985]. The dissolution of calcite in coastal plain aquifers results in the replacement of Na with Ca on the exchanging substrate (Ex) as follows:



[15] This process would produce a Na-HCO<sub>3</sub> type water with high Na/Cl molar ratios (Table 2). Similar Na-HCO<sub>3</sub> type groundwaters occur in the Atlantic coastal plain

[Schwartz and Zhang, 2003] and the Milk River aquifer in Canada [Hendry and Schwartz, 1990]. The abundance of glauconite [Cook, 1997] in marine coastal plain sediments of Alabama suggests it may be the primary medium for ion exchange. Glauconite is also the dominant exchanging medium identified in the Maryland coastal plain [Chapelle and Knobel, 1983].

[16] Ion exchange between clay substrates and groundwater is a selective process. A specific sequence of ion exchange is expected resulting from competition between water dipoles and negative surface exchange sites on clay substrates. Chapelle and Knobel [1983] indicated that cations with smaller hydrated radii are held more strongly to exchange sites than those with larger hydrated radii. Moreover, bonded divalent cations tend to be more stable than bonded monovalent cations. The observed sequential peaks of cations (Figure 3) are generally consistent with the order of cations competing for exchange sites:  $\text{Ca}^{+2} > \text{Mg}^{2+} > \text{K}^+ > \text{Na}^+$ . The sequences of Mg and Ca are not so widely separated (Figure 3) probably because both have two positive charges and are so similar in size. Our geochemical data suggest that the dominant water-sediment-bacteria interactions in the shallow Alabama coastal plain include a combination of microbially mediated Fe(III) and Mn(IV) reduction and ion exchange between groundwater and clay minerals.

#### 4.2. Carbon Isotope Compositions of Groundwater and Carbonate Minerals

[17] Carbon isotopic signatures of groundwaters (Table 2) and coexisting authigenic minerals may be used to interpret relative influences of various geochemical reactions (e.g., bacterial Fe(III)-reduction, methanogenesis, and abiogenic ion exchange) that control bulk water chemistry. Because both bacterial Fe(III)-reduction and ion exchange processes can raise the pH and alkalinity of groundwater, carbon isotopic compositions can be used as a fingerprint that

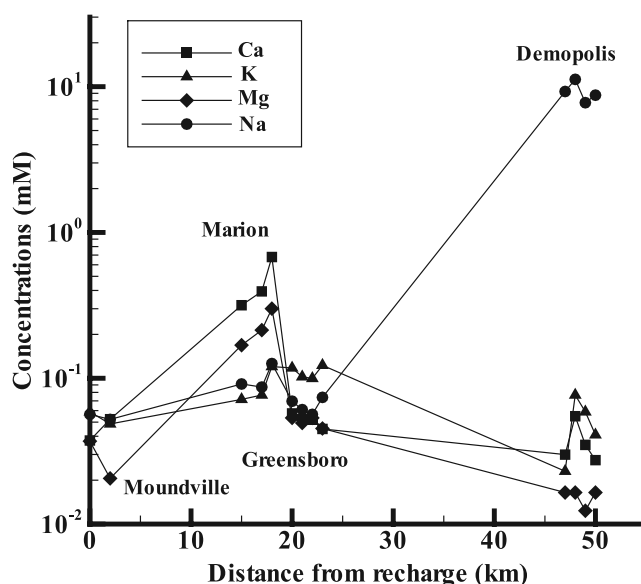


**Figure 3.** Concentrations of dissolved Ca, Mg, K, and Na in the Eutaw aquifer as function of distance along a flow path in western Alabama.

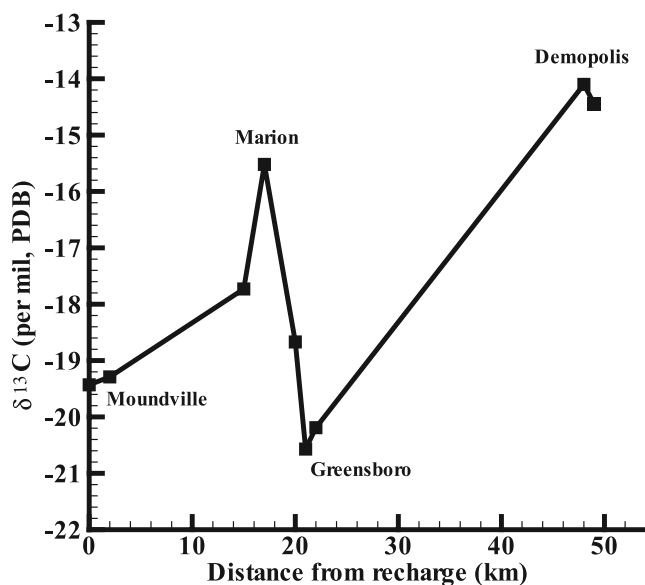


**Figure 4.** The  $\delta^{13}\text{C}$  ratios (‰, PDB) of Eutaw groundwater as a function of distance along a flow path in western Alabama.

may indicate the relative dominance of each process. Photosynthesis enriches biologically synthesized organic compounds in  $^{12}\text{C}$ . Dissolved carbonate formed from the bacterial oxidation of organic compounds is typically depleted in  $^{13}\text{C}$  ( $< -15\%$ , PDB) relative to an inorganic carbon source such as marine carbonate rocks ( $\approx 0\%$ ) [Faure, 1997].

[18] The  $\delta^{13}\text{C}$  compositions of dissolved inorganic carbon (DIC) in Eutaw groundwater (Table 2) range from  $-20.6\%$  to  $-14.1\%$  (PDB) in the study area. The relatively low  $\delta^{13}\text{C}$  values indicate that the reactions controlling alkalinity mostly involve biogenic sources, including the dissolution of biogenic soil  $\text{CO}_2$  and oxidation of organic matter. We also analyzed the carbon isotopic composition of authigenic siderite and rhodochrosite collected from core samples of Marion and Demopolis wells (Table 3). The depleted  $\delta^{13}\text{C}$  values ( $-15.4$  and  $-14.3\%$  of samples 6567 and 2052, respectively) of carbonate solids also implicate organic carbon in the emplacement of these biogenic minerals. These values are significantly lower than those would be expected in marine carbonates, which normally range  $-4$  to  $+4\%$  [Faure, 1997].

[19] It is intriguing that isotopically heavier DIC (i.e., higher  $\delta^{13}\text{C}$  values) generally correlated with elevated Fe

and Mn concentrations and high pH values in Marion and Demopolis groundwaters (Figure 4). This remarkable result is unexpected because metabolism of Fe reducing bacteria would add isotopically lighter DIC into groundwater. This apparent contradiction indicates that microbial reduction of Fe(III) and subsequent biochemical reactions may affect the processes of DIC speciation and carbon isotopic fractionation. The speciation of various carbon species including dissolved  $\text{CO}_2$ ,  $\text{H}_2\text{CO}_3$ ,  $\text{HCO}_3^-$  and  $\text{CO}_3^{2-}$  of DIC is pH-dependent. At low pH ( $< 5$ ), DIC is dominated by dissolved  $\text{CO}_2$ , whereas at high pH ( $> 8$ ), DIC is comprised primarily of  $\text{HCO}_3^-$  and  $\text{CO}_3^{2-}$ . At  $25^\circ\text{C}$ ,  $\text{HCO}_3^-$  and  $\text{CO}_3^{2-}$  are enriched in  $^{13}\text{C}$  by about  $9\%$  relative to dissolved  $\text{CO}_2$  [Clark and Fritz, 1997]. Thus as bacterial iron reduction raises pH (reaction 2), the concentration of dissolved  $\text{CO}_2$  decreases and that of  $\text{HCO}_3^-$  increases concurrently; this would lead to higher DIC  $\delta^{13}\text{C}$  values. It is also likely that bacteria may utilize lighter  $^{12}\text{C}$  to form biogenic carbonate minerals, making the remaining water relatively enriched in  $^{13}\text{C}$ . The latter interpretation, however, requires further investigation into the bacterial isotope fractionation of biogenic carbonate solids during biomineralization. Alternatively, dissolution of inorganic calcite during ion exchange, degassing of  $\text{CO}_2$  and  $\text{CH}_4$ , and methanogenesis would cause further enrichment in  $^{13}\text{C}$  of DIC.

#### 4.3. Biomineralization in Fe-Rich Sediments

[20] Petrographic and SEM-based energy-dispersive analyses reveal the mineralogy, chemical compositions, particle size, and authigenic nature of solids precipitated from Fe- and Mn-rich groundwater. Analyzed cutting samples were chosen from proximal wells (Table 3) in the same cities (Moundville, Marion, Greensboro, and Demopolis) where Fe-rich groundwaters occur. Analysis of well-cutting samples was first attempted using X-ray diffraction, but the extremely high abundance of quartz subdued any discernable mineral peaks. Petrographic thin section analysis shows the presence of a variety of primary and secondary minerals. Quartz is abundant and ubiquitous in all samples followed by the second most abundant mineral, muscovite, which is found in all samples except 4573 and 6567 from Marion and Demopolis. Glauconite (Figure 5a) is also abundant in nearly all samples with the exception of sample 1239 from Moundville.

[21] Biogenic minerals such as pyrite (Figure 5b) and botryoidal forms of both rhodochrosite and siderite (Figures 5c, 5d, 6a, and 6b) are present in well-cutting samples. Authigenic pyrite is found in samples 2052, 3637, and 6567 corresponding with Fe-rich zones in the Marion and Demop-

**Table 3.** Well-Cutting Samples and Mineralogy Analyzed in the Study Area<sup>a</sup>

GSA Number	Well Name	County	Distance From Recharge, km	Sample Interval (Feet Below Surface)	Mineralogy
1239	Moundville 1	Hale	0–2	249–272	qz + mus + py
4573	Marion TW1	Perry	17–18	608–637	qz
2052	Marion TW3	Perry	17–18	729–752	qz + mus + gla + py + sid + rho
1095	Greensboro 2	Hale	20–23	702–712	qz + mus + gla
3637	Demopolis 1	Marengo	47–50	896–919	qz + mus + gla + py
6567	Demopolis 5	Marengo	47–50	1102–1118	qz + mus + py + sid + rho

<sup>a</sup>Samples are identified by Geological Survey of Alabama (GSA) number. Abbreviations: quartz, qz; muscovite, mus; pyrite, py; glauconite, gla; siderite, sid; rhodochrosite, rho.

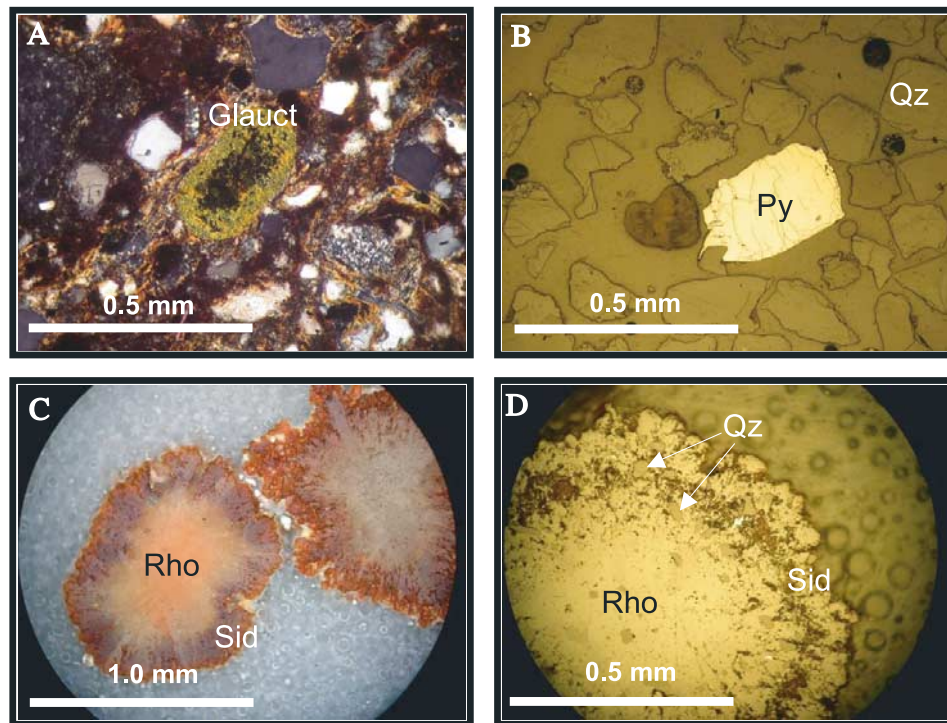


**Figure 5.** Photomicrographs of minerals in the Eutaw Formation. Thin sections of (a) glauconite (Glauct) (cross-polars), and (b) biogenic pyrite (Py) (reflected light) along with polished thick sections of biogenic rhodochrosite (Rho) rimmed with siderite (Sid) in (c) reflected light and (d) reflected light with varied polarization.

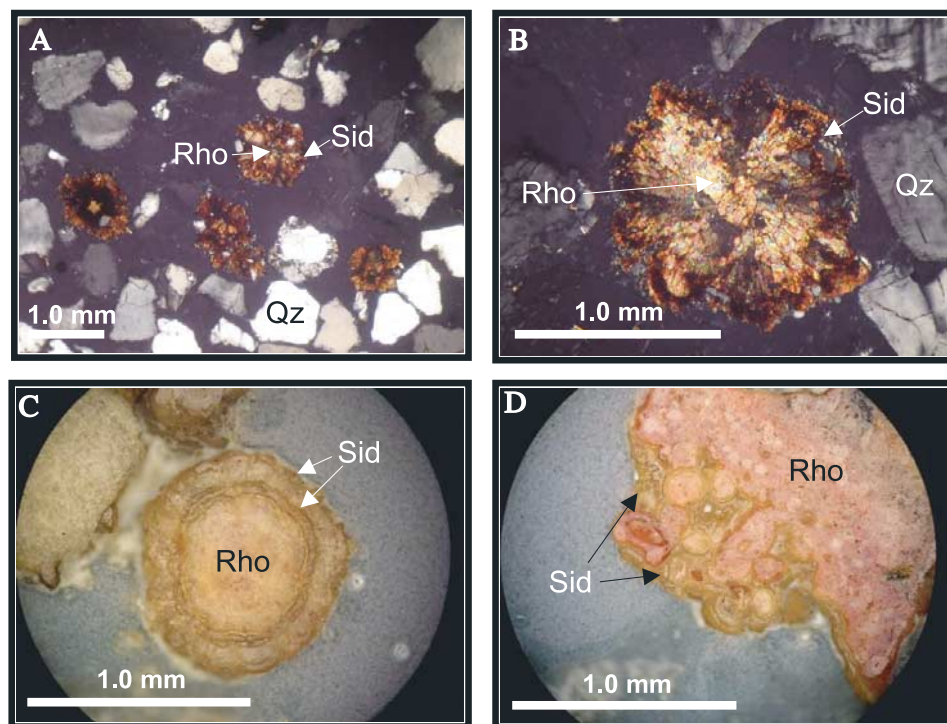


**Figure 6.** Photomicrographs of minerals in the Eutaw Formation and Paleozoic aquifer. (a, b) Biogenic rhodochrosite (Rho) and siderite (Sid) grains (cross-polarized light) from the Eutaw aquifer. (c, d) are polished thick sections (reflected light) of biogenic rhodochrosite (Rho) and siderite (Sid) from the Paleozoic aquifer [from *Saunders and Swann, 1992*].

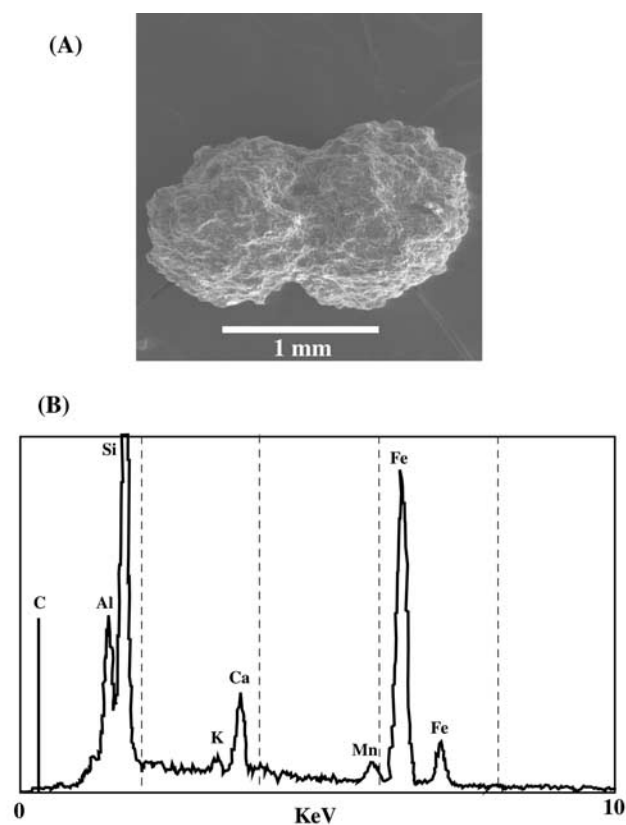


**Figure 7.** (a) SEM image and (b) energy dispersive x-ray (EDAX) spectra of biogenic siderite/rhodochrosite doublets from Demopolis well 5 (GSA 6567).

olis areas. Rhodochrosite and siderite occur together in Fe-rich wells (2052 and 6567) as spheroids ( $>1.0$  mm) in which rhodochrosite forms the center and siderite forms an outer rind, which is consistent with the sequence of mineral precipitation predicted by the geochemical modeling (see next section). Thus the reduction of Fe(III) oxides and the formation of siderite occurs after Mn reduction is almost completed. These spheroids are locally more abundant in Fe- and Mn-rich wells from Marion (2052) and Demopolis (6567). The occurrence of joined doublets (Figure 7a) of spherical iron carbonates may be attributed to the merging growth of adjacent minerals from groundwater. EDAX of these spheroids consistently results in peaks for Fe, Mn, C, along with minor Ca (Figure 7b). Peak heights and quantities for metals suggest that siderite is the predominant mineral. Inclusion of quartz grains within the structure of rhodochrosite and siderite grains also provides textural evidence that these minerals are authigenic (Figure 5d).

[22] The precipitation and dissolution of various Fe carbonate and sulfide minerals may control the mobility of Fe, Mn, and other metals (e.g., Sr, Ba, As) in groundwater. Similar authigenic (biogenic) siderite and rhodochrosite minerals were found in Mississippi coastal plain sediments [Saunders and Swann, 1992] (Figures 6c and 6d) and alluvial sediments in India and Bangladesh [Pal et al., 2002; Sengupta et al., 2004; Turner, 2006]. The actual biogeochemical processes by which bacteria contribute to biomineralization in the Fe-rich sediments remain poorly under-

stood. Previous studies [e.g., Lowenstam, 1981; Konhauser, 1998; and Fredrickson et al., 1998] have shown that biogenic minerals can form in both direct and indirect contact with bacteria. Direct contact, known as biologically controlled mineralization, is able to occur both intracellularly and extracellularly as bacteria electrostatically bind metals to their anionic cell wall surfaces providing nucleation sites for physiologically essential minerals [Mann, 1983; Konhauser, 1998]. Laboratory studies [e.g., Roden and Lovley, 1993] have shown biomineralization through direct enzymatic reduction of Fe(III) into  $\text{FeCO}_3$  by *Desulfuromonas acetoxidans* in the presence of  $\text{HCO}_3^-$ -rich media.

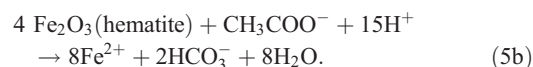
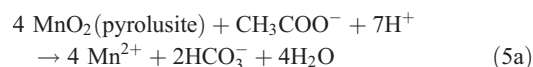
[23] Biologically induced mineralization is the incidental mineral formation due to release of byproducts into solution by bacterial activity and is also the dominant process among bacteria [Konhauser, 1998]. This process characteristically forms environmentally dependent biominerals based on available materials surrounding the bacteria. In this manner, mineral size is not limited by association with the bacterial cell wall (nanometers to micrometers [Konhauser, 1998]) and is potentially able to reach greater sizes as those carbonates observed in this study ( $>1$  mm, Figure 5c). Because levels of Fe(II), Mn(II), and  $\text{HCO}_3^-$  are abundant in the Eutaw aquifer, biomineralization of  $\text{FeCO}_3$  and  $\text{MnCO}_3$  observed in Marion and Demopolis wells may be biologically induced as in the following equation:



[24] In this reaction, the presence of Fe(II), bicarbonate, and hydroxyl ions released from bacterial Fe(III) reduction will directly precipitate siderite.

#### 4.4. Bacterial Reduction of Fe(III) and Mn(IV) Oxides

[25] We used GWB [Bethke, 1996] to trace the sequence of biogeochemical reactions that occurs during the bacterial Fe(III) and Mn(IV) oxide reduction, which subsequently induces the precipitation of Fe carbonate and sulfide minerals. The purpose of the modeling is to provide insights on the sequence of mineral reactions during the reductive dissolution of Fe and Mn oxides and how mineral reactions affect metal mobility in groundwater. We begin by equilibrating an Alabama coastal plain groundwater upstream of an iron reduction zone under aerobic conditions at 25°C. The calculation uses the water chemical data collected from the Eutaw aquifer in Moundville (well MV1) and assumes the initial concentrations of Fe and Mn reflect equilibrium with hematite ( $\text{Fe}_2\text{O}_3$ , a proxy of Fe(III) oxyhydroxides) and pyrolusite ( $\text{MnO}_2$ , a proxy for Mn(IV) oxyhydroxides) in the sediments. The model then simulates the geochemical effects of titration of organic matter into the system. We consider transformation of pyrolusite and hematite by the following redox reaction:



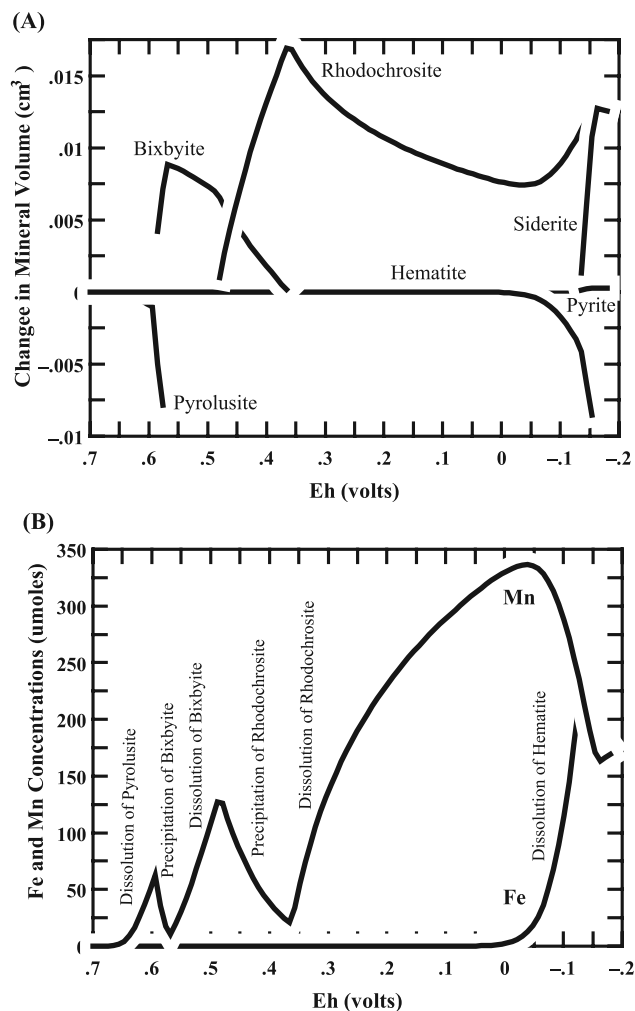
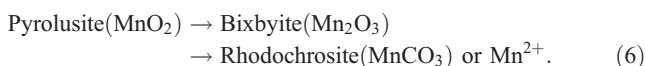


**Figure 8.** (a) Predicted sequence of mineralogical reactions resulting from bacteria reduction of Fe and Mn oxides in equilibrium with Moundville groundwater near the Eutaw aquifer outcrop. The plot shows changes in mineral volume as acetate is titrated into the system and Eh decreases with time. Positive changes indicate precipitation, and negative changes show dissolution. (b) Calculated total Mn and Fe concentrations in fluid predicted by the same reaction path model.

[26] In the simulation, fluid reactants containing 500  $\mu\text{mol}$  of acetate ( $\text{CH}_3\text{COO}^-$ ) displace existing fluid from the system and the values of Eh slide from +700 mV to -200 mV over the reaction path.

[27] The predicted mineral reactions of manganese and iron oxides (Figure 8a) follow the well-known Ostwald's step rule [Morse and Casey, 1988; Norden and Sibley, 1994]. Pyrolusite in the initial system first becomes thermodynamically unstable during bacterial reduction and transforms over time to a sequence of progressively more stable manganese minerals and species (Figure 8a) at lower oxidation states,



[28] Once the reduction of Mn minerals has nearly been completed, the iron redox reactions start (Figure 8a) and

hematite ( $\text{Fe}_2\text{O}_3$ ) begins to dissolve to form more stable siderite ( $\text{FeCO}_3$ ) or pyrite at low oxidation states. The progression of calculated redox potential and pH values are projected in the activity diagrams showing various stability fields of Mn and Fe minerals and species (Figure 9). The reduction of Fe(III) oxides occurs under more reducing conditions than Mn minerals. At the later stage of the

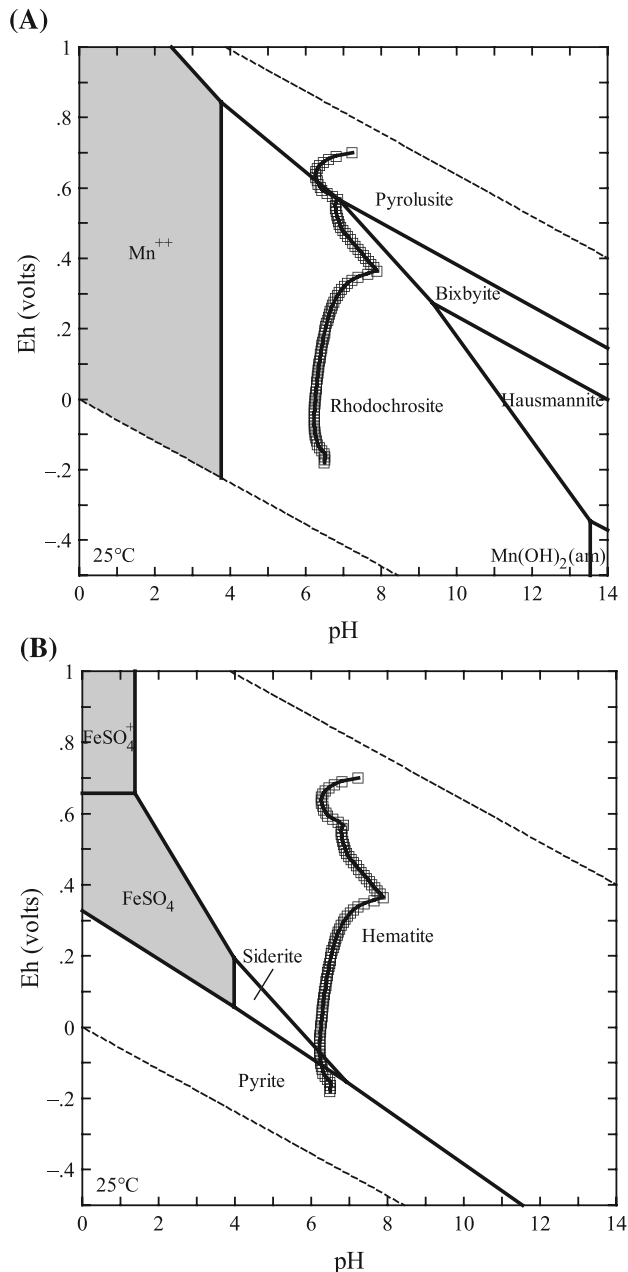


**Figure 9.** Eh-pH diagram calculated for average geochemical conditions in (a) Mn-HCO<sub>3</sub>-H<sub>2</sub>O and (b) Fe-HCO<sub>3</sub>-H<sub>2</sub>O systems. Activity of dissolved species:  $\text{Fe}^{2+} = 10^{-2}$ ,  $\text{Mn}^{2+} = 10^{-2.5}$ ,  $\text{SO}_4^{2-} = 10^{-3}$ , and  $\text{HCO}_3^- = 10^{-2}$  mol. The reaction trace of bacterial Mn and Fe reduction in Figure 8 is projected as open squares onto the diagram. The reaction trace shows the sequence of mineral reactions during the reductive dissolution of Mn and Fe oxides as Eh decreases. This activity diagram was generated by the Geochemist's Workbench [Bethke, 1996].

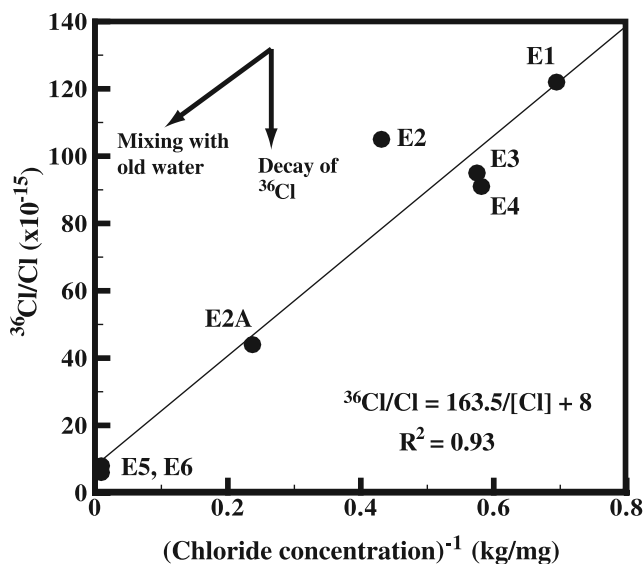


**Figure 10.** Regression curve for  $^{36}\text{Cl}/\text{Cl}$  ratios and Cl concentrations of groundwater from the Eutaw aquifer in western Alabama [after Penny *et al.*, 2003]. The two arrows represent radioactive decay and mixing with old groundwater that can change  $^{36}\text{Cl}/\text{Cl}$  ratios and Cl concentrations.

reaction, reduced metal species also combine with  $\text{HCO}_3^-$  released from organic sources to form minerals such as rhodochrosite ( $\text{MnCO}_3$ ) and siderite ( $\text{FeCO}_3$ ). Under highly reducing conditions, reduced aqueous  $\text{Fe}^{2+}$  reacts with  $\text{H}_2\text{S}$  to form pyrite, which can remove trace elements such as Co, Ni, and As from groundwater by coprecipitation [Saunders *et al.*, 1997; Lehner *et al.*, 2006]. It should be noted that Fe- and Mn-rich groundwaters downstream from Moundville are actually saturated with siderite and rhodochrosite [Penny *et al.*, 2003]. Our petrographic, SEM, and EDAX studies confirmed the precipitation of biogenic siderite, rhodochrosite, and pyrite in Fe- and Mn-rich wells (Figures 5 and 6). Figure 8b shows the calculated Mn and Fe concentrations in fluid over the same reaction path. It clearly demonstrates how the precipitation and dissolution of various Mn- and Fe-minerals control the mobility of metals in groundwater. Rapid rise and fall of metal concentrations observed a short distance along the flow path (Figure 2) from the recharge zone may be explained by the transformation of various iron and manganese minerals. Moreover, the modeling results imply that the transformation of iron and manganese minerals could control mobility of other metals such as arsenic in coastal plain aquifers and requires continued investigation.

[29] It should be noted that the field data show no truly strong correlation among Fe, Mn, pH, alkalinity, and  $\delta^{13}\text{C}$  values of DIC because the chemical evolution of groundwater can be affected by various biogeochemical reactions (i.e., bacterial iron reduction, sulfate reduction, methanogenesis) as well as mineral precipitation and dissolution. A perfect correlation among these parameters might be expected if a groundwater flow zone is dominated by a single biogeochemical or mineral reaction. Recent studies [e.g., Park *et al.*, 2006; Turner, 2006], however, found no compelling evidence that the respiration of one type of microbes would exclude others from any of an aquifer's

redox zones. This implies that a change of the groundwater from high-Fe into low-Fe facies over a short distance (Figure 2) may result from a minor adjustment in the balance between the activities of iron and sulfate reducers or biotransformation of metals-bearing minerals. For example, bacterial-induced precipitation of siderite will preferentially remove Fe relative to other ions in groundwater. Bacterial sulfate reduction and precipitation of iron sulfides could strip  $\text{Fe}^{2+}$ ,  $\text{SO}_4^{2-}$ ,  $\text{H}^+$ , and perhaps other trace elements (by coprecipitation) from solution in different ratios.

#### 4.5. The $^{36}\text{Cl}$ Transport Modeling and Residence Time

[30] Radioactive isotope data provide quantitative information on the age of groundwater and thus may be used to characterize flow directions and velocities. Field measured  $^{36}\text{Cl}/\text{Cl}$  ratios consistently decrease along the flow path with values ranging from  $122 \times 10^{-15}$  near outcrops to  $6 \times 10^{-15}$  downdip near Demopolis (Figure 10). Higher  $^{36}\text{Cl}/\text{Cl}$  ratios near the recharge area are representative of young groundwater that has a high atmospheric  $^{36}\text{Cl}$  signature ( $>100 \times 10^{-15}$ ) [Davis *et al.*, 2000] but with little  $^{35}\text{Cl}$ .

[31] We used a basin hydrology model Basin2 to simulate the decay and transport of  $^{36}\text{Cl}$  along the flow path in western Alabama. The model assumes that the surface of the coastal plain is open to fresh water recharge with a constant  $^{36}\text{Cl}/\text{Cl}$  ratio of  $125 \times 10^{-15}$ , in the same range as those measured in the field [Davis *et al.*, 2000]. Basin2 can consider additional sources of  $^{36}\text{Cl}$  other than the input from atmospheric recharge, primarily by neutron activation of  $^{35}\text{Cl}$  (i.e.,  $^{35}\text{Cl} + n \rightarrow ^{36}\text{Cl}$ ). In the activation reaction, decay of uranium and thorium in sediments releases neutrons that collide with  $^{35}\text{Cl}$  atoms that are present in groundwater or contained in evaporite minerals. Production of  $^{36}\text{Cl}$  by this process, however, is usually far outweighed by the natural decay of the isotope. Only under certain conditions where aquifer sediments contain abundant uranium, thorium, and evaporite minerals, which provide  $^{35}\text{Cl}$ , is such a process important. The Eutaw Formation is not known to contain any appreciable amounts of uranium, thorium, or evaporite minerals, thus neutron activation is not considered in the model. Inclusion of neutron production of  $^{36}\text{Cl}$  in the model would slightly increase calculated  $^{36}\text{Cl}$  concentrations or underestimate the residence time of groundwater. Radioactive isotopes such as  $^{36}\text{Cl}$  can also diffuse into groundwater along the basin's bottom basement boundary. This input source was also turned off because thick piles ( $>3$  km) of coastal plain sediments likely prevent any significant upward diffusive transport of  $^{36}\text{Cl}$  into the shallow Eutaw aquifer.

[32] In the model, two critically sensitive variables may significantly affect  $^{36}\text{Cl}$  transport along the flow path: (1) the permeability ( $k$ ) of sand in the Eutaw aquifer and (2) the diffusion through the upper confining unit (i.e., the Selma Group) that separates the Eutaw aquifer from surface sources. Permeability of sediments affects advective and dispersive transport of  $^{36}\text{Cl}$  through sediments and influences the residence time of groundwater in the aquifer. The coefficient of hydrodynamic dispersion ( $D$ ) for  $^{36}\text{Cl}$  transport can be calculated as

$$D_L = \alpha_L v_x + D^* \quad (7a)$$

$$D_T = \alpha_T v_z + D^* \quad (7b)$$

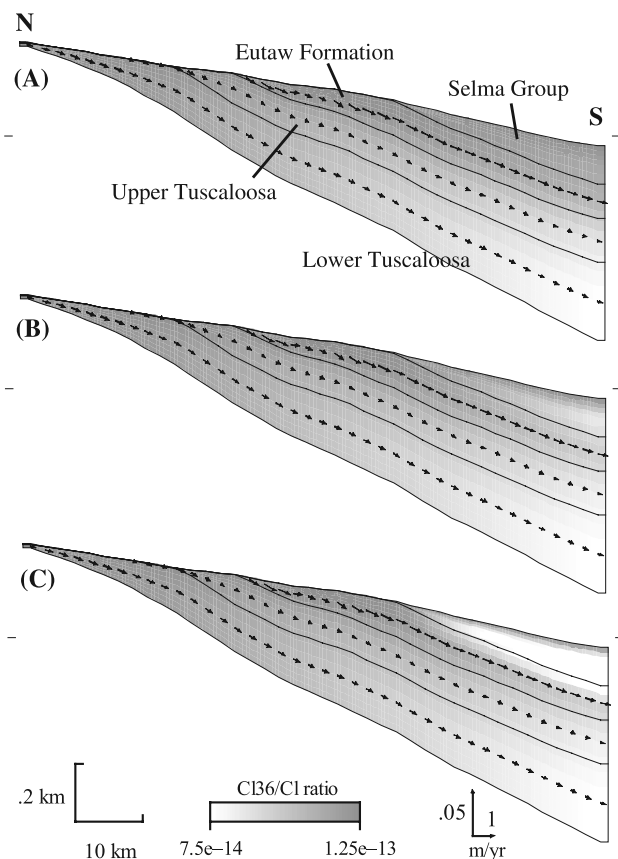


**Figure 11.** Calculated  $^{36}\text{Cl}/\text{Cl}$  ratios along the Eutaw flow path (second stratigraphic unit from top) with permeability set at  $k = 0.1$  darcies. Arrows show the predicted flow velocities. (a)  $D^* = 10^{-4}$ , (b)  $D^* = 10^{-5}$ , and (c)  $D^* = 10^{-6}$   $\text{cm}^2/\text{s}$ .

[33] Here  $D_L$  and  $D_T$  are the longitudinal and transverse coefficients of hydrodynamic dispersion,  $\alpha_L$  and  $\alpha_T$  are the dynamic dispersivity, and  $v_x$  and  $v_z$  are the average linear groundwater velocity in  $x$  and  $z$  directions. According to equation (7), diffusion coefficient ( $D^*$ ) becomes important in low-permeability confining aquitards where the average linear groundwater velocity ( $v$ ) is very small. The diffusion coefficient ( $D^*$ ) of the surficial confining sediments (Selma Group) could affect the amount of  $^{36}\text{Cl}$  in surface water ( $^{36}\text{Cl}/\text{Cl} = 125 \times 10^{-15}$ ) diffusing downward into the Eutaw aquifer. Although the Selma Group is composed primarily of relatively impermeable carbonate material (i.e., limestone and chalk [Mallory, 1993]), the thin strata due to pinch-out at the southwestern terminus of the study area (maximum thickness  $< 140$  m), may have some potential for downward diffusion of surface water.

[34] Our sensitivity analysis first explored how variations in  $D^*$  may affect  $^{36}\text{Cl}$  concentrations in the aquifer. The Eutaw aquifer had a constant permeability value of 0.1 darcy (1 darcy =  $10^{-8}$   $\text{cm}^2$ ) in the simulations. In three sets of numerical experiments, an increase of from  $10^{-6}$  to  $10^{-4}$  ( $\text{cm}^2/\text{s}$ ) results in a noticeable increase in  $^{36}\text{Cl}/\text{Cl}$  ratios in the underlying Eutaw aquifer (Figure 11). The calculation that assumes high diffusion coefficient shows little variation in  $^{36}\text{Cl}$  along the aquifer as diffusion from surface water

overwhelms isotopic transport and natural decay (Figure 11a). A reduction in vertical diffusion (Figures 11b and 11c) would allow  $^{36}\text{Cl}$  concentrations to decrease significantly down-dip by natural decay along the flow path. The residence time of groundwater, inferred from calculated  $^{36}\text{Cl}$  concentrations, increases with increasing travel distance along the flow path (Figure 12). Calculations allowing a high degree of diffusion of  $^{36}\text{Cl}$  from surface sources result in “younger” isotope ages. It should be noted that the variations of  $D^*$  of the overlying confining Selma Group only affect calculated  $^{36}\text{Cl}/\text{Cl}$  ratios or residence time of groundwater in the confined portion of the Eutaw aquifer (Figure 13).

[35] Simulations were repeated for decreasing permeability of 0.01 darcy at three values of  $10^{-4}$ ,  $10^{-5}$ , and  $10^{-6}$   $\text{cm}^2/\text{s}$ . Lower permeability and flow rates (which allow longer decay time given the same travel distance) result in much lower  $^{36}\text{Cl}$  ( $^{36}\text{Cl}/\text{Cl}$  ratios  $< 10 \times 10^{-15}$ ) concentrations in groundwater beyond the recharge area (Figure 14). Owing to slower flow rates at a lower permeability, the predicted residence times of groundwater are older than those calculated at higher flow rates (Figure 12). In summary, lower aquifer permeability (0.01 darcy) in the Eutaw Formation, in conjunction with reduced diffusion coefficients ( $10^{-6}$   $\text{cm}^2/\text{s}$ ) of the Selma Group, yields  $^{36}\text{Cl}/\text{Cl}$  ratios that closely match field measured data of  $^{36}\text{Cl}$  (Figure 13). Such low permeability ( $k = 10^{-2}$  darcies) and diffusion coefficient values ( $10^{-6}$   $\text{cm}^2/\text{s}$ ), however, do not represent realistic hydrologic characteristics of coastal plain sediments, and are not likely the reason for the large decrease in  $^{36}\text{Cl}/\text{Cl}$  ratios. The lithology of the Eutaw Formation is known to be composed primarily of fine to medium-grained sand, with localized clay zones for silty and fine sands, and potentially greater values in areas where sands are coarser and well sorted. Horizontal permeability

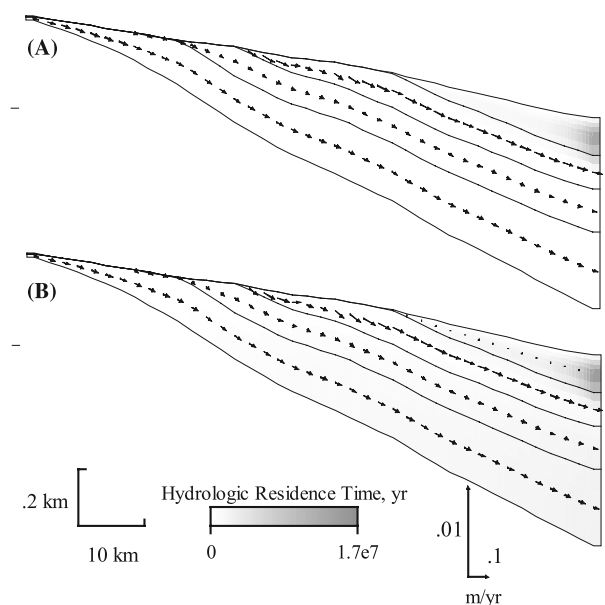


**Figure 12.** Calculated hydrologic residence times along the Eutaw flow path with permeability set at (a)  $k = 0.1$  darcies and (b)  $k = 0.01$  darcies. In both cases,  $D^*$  values are set at  $10^{-5}$   $\text{cm}^2/\text{s}$ .

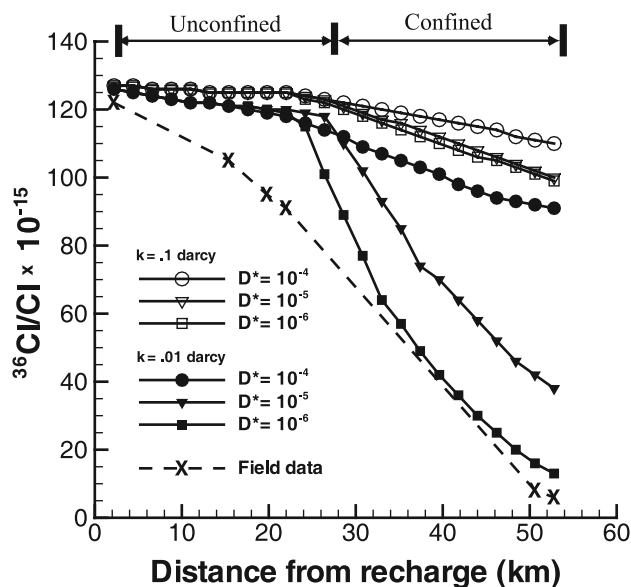


**Figure 13.** Calculated  $^{36}\text{Cl}/\text{Cl}$  ratios along the flow path resulting from variable sand permeability ( $k$ ) and diffusion coefficient ( $D^*$ ). Model configurations with low  $k$  and  $D^*$  values (solid symbols) closely resemble field data (crosses). Higher flow rates near the outcrop or unconfined portion of the aquifer lead to slow decay of  $^{36}\text{Cl}$ . Small hydraulic gradient and flow rates in the confined portion of the aquifer results in a greater decay of  $^{36}\text{Cl}$  over the same travel distance.

along the layered stratigraphy is best calculated as an arithmetic average [Deming, 2002]. The arithmetic method gives average permeability near that of a more permeable unit (0.1 to 1 darcy) over a wide range of mixing. Lower diffusion coefficients ( $<10^{-5}$  cm<sup>2</sup>/s) may be probable given the relatively impermeable nature of carbonates composing the Selma Group, but field measurements of diffusive properties do not exist and can only be estimated from laboratory data ( $\approx 10^{-4}$  cm<sup>2</sup>/s) [Freeze and Cherry, 1979]. We interpret that significant mixing with old groundwater (with little  $^{36}\text{Cl}$  but high Cl concentrations) downdip is mainly responsible for the rapid decrease of  $^{36}\text{Cl}/\text{Cl}$  ratios observed in the field. The results suggest that mixing of older groundwater has significantly lowered  $^{36}\text{Cl}/\text{Cl}$  ratios of groundwater downdip. The use of  $^{36}\text{Cl}/\text{Cl}$  ratios in groundwater dating or flow rate calculations must be interpreted with great caution.

## 5. Conclusions

[36] This research integrates geochemical data and numerical modeling techniques to analyze complex water-sediment-bacteria interaction and hydrologic transport in Alabama coastal plain aquifers. Results indicate that both inorganic (ion exchange) and bacterially mediated (bacterial Fe(III)- and Mn(IV)-reduction) processes work together to produce groundwater with elevated levels of trace metals and cations that correlate with high pH and alkalinity. Geochemical correlations, reducing Eh values, and the presence of authigenic carbonate solids and their light  $\delta^{13}\text{C}$  signatures support the hypothesis that elevated Fe

and Mn concentrations and biomineralization are derived from bacterial Fe(III) and Mn(IV) reduction. The presence of Fe(III)-reducing bacteria in Fe and Mn-rich Eutaw groundwaters from the Marion and Demopolis city wells [Penny *et al.*, 2003] further supports these biogeochemical reactions. Most Fe-reducing microorganisms require sources of ferric iron and carbon to grow and metabolize. Fe (III) hydroxides (common in the coastal plain aquifer sediments) such as goethite, hematite, and ferrihydrite can be used as a ferric iron source for these organisms. It is likely that other heterotrophic bacteria such as sulfate reducers are also present in the Eutaw aquifer, as suggested by the presence of biogenic pyrite.

[37] The predicted mineralogical reactions under progressively reducing conditions show that Fe reduction proceeds after the Mn reduction reactions are completed. Fe and Mn oxides in the initial system are transformed by heterotrophic anaerobic bacteria to a sequence of progressively more stable minerals and species at lower oxidation states. At the later stage of the reaction, reduced metal species also combine with  $\text{HCO}_3^-$  released from organic sources to form minerals such as rhodochrosite ( $\text{MnCO}_3$ ) and siderite ( $\text{FeCO}_3$ ). Reduced aqueous  $\text{Fe}^{2+}$  reacts with  $\text{H}_2\text{S}$  to form pyrite under reducing conditions. Petrographic, SEM, and EDAX studies of well-cutting samples confirmed the precipitation of biogenic siderite, rhodochrosite, and pyrite in the Fe- and Mn-rich wells. The modeling results and

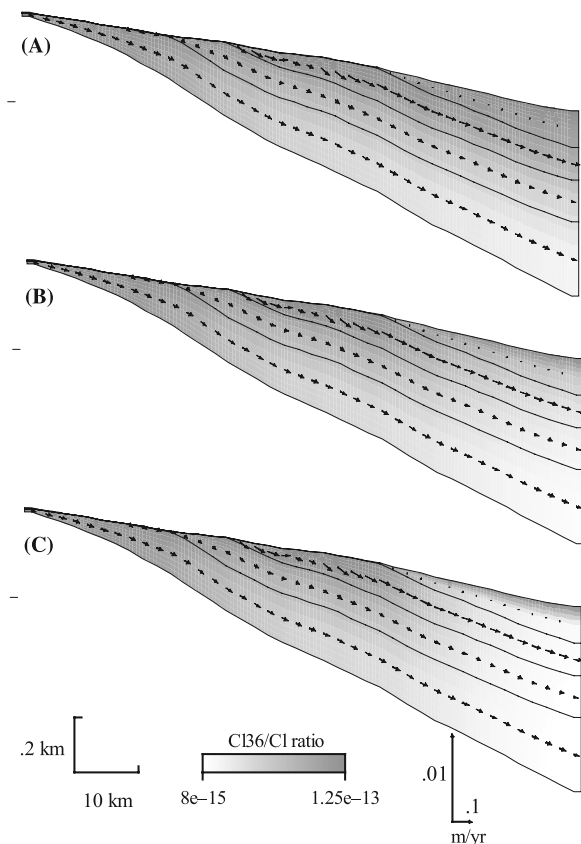


**Figure 14.** Calculated  $^{36}\text{Cl}/\text{Cl}$  ratios along the Eutaw flow path (second stratigraphic unit from top) with permeability set at  $k = 0.01$  darcies. (a)  $D^* = 10^{-4}$ , (b)  $D^* = 10^{-5}$ , and (c)  $D^* = 10^{-6}$  cm<sup>2</sup>/s.

geologic data indicate that the precipitation and dissolution of various Mn- and Fe-minerals control the mobility of metals in groundwater; biotransformation of these minerals could be responsible for rapid rise and fall of metal concentrations observed over short distance along the flow path.

[38] Ion exchange is also responsible for geochemical alteration of groundwater by increasing major ion concentrations and pH and alkalinity values. Such a process is characterized by sequential ion peaks ( $\text{Ca}^{+2}$ ,  $\text{Mg}^{+2}$ ,  $\text{K}^{+}$ , and  $\text{Na}^{+}$ ) observed along the flow path. Results of  $^{36}\text{Cl}$  transport modeling indicate that the rapid decrease of  $^{36}\text{Cl}$  along the flow path cannot solely result from natural isotope decay, and that an alternative mechanism such as mixing with older, saline groundwater with high Cl concentrations but with little or no  $^{36}\text{Cl}$  is important. Substantial mixing can lower  $^{36}\text{Cl}/\text{Cl}$  ratios in groundwater and thus the interpretation of groundwater ages based on field data could lead to an underestimation of groundwater recharge rates.

[39] This study demonstrates that quantitative geochemical and hydrological transport models can be used in conjunction with field data to assess chemical evolution and complex water-sediment-bacteria interaction in regional groundwater systems. Our results show that a wide variety of geochemical and microbial processes, including such diverse phenomena as bacterial metal reduction, biomineralization, diagenesis, ion exchange, and transport and fractionation of isotopes, are the results of reactive transport in the subsurface. Future research should be directed toward the biogeochemical evolution of regional flow systems which involves diverse processes including fluid flow, chemical and biological reactions, and solute transport operating at differing time and distance scales. Numerical models can be used qualitatively or quantitatively to provide insight into complex biogeochemical reactions and hydrological transport processes that significantly modify water chemistry over both local and regional scales.

[40] **Acknowledgments.** This research was partly supported by grants from the National Science Foundation (NSF-0352936 and 0445250) and the Petroleum Research Fund, administered by the American Chemical Society under ACS-PRF 33111-GB8 (to Ming-Kuo Lee). We thank Roger Lee, Marlon Cook, and Charles Smith for many helpful discussions on hydrogeology and stratigraphy of the study area. Keith Hackley and Huei-Hwa Huang of the Illinois State Geological Survey for helping make isotopic measurements, and Craig Bethke (University of Illinois) for providing the Basin2 computer software for basin hydrology and  $^{36}\text{Cl}$  transport modeling. Additionally, constructive comments by Alan Fryer and two anonymous reviewers greatly improved this paper.

## References

Alley, W. M., R. W. Healy, J. W. LaBaugh, and T. E. Reilly (2002), Flow and storage in groundwater systems, *Science*, 296, 1985–1990.

Appelo, C. A. J. (1994), Cation and proton exchange, pH variations, and carbonate reactions in a freshening aquifer, *Water Resour. Res.*, 30, 2793–2805.

Back, W., and B. B. Hanshaw (1970), Comparison of chemical hydrogeology of the carbonate peninsulas of Florida and Yucatan, *J. Hydrol.*, 10, 330–368.

Barcelona, M. J., T. R. Holm, M. R. Schock, and G. K. George (1989), Spatial and temporal gradients in aquifer oxidation-reduction conditions, *Water Resour. Res.*, 25, 991–1003.

Barker, R. A., and M. Pernik (1994), Regional hydrology and simulation of deep ground-water flow in the southeastern coastal plain aquifer system in Mississippi, Alabama, Georgia, and South Carolina, *U.S. Geol. Surv. Prof. Pap.*, 1410-C, 1–87.

Bentley, H. W., F. M. Phillips, S. N. Davis, M. A. Habermehl, P. L. Airey, G. E. Calf, D. Elmore, H. E. Gove, and T. Torgersen (1986), Chlorine 36

dating of very old ground water: I. The Great Artesian basin, Australia, *Water Resour. Res.*, 22, 1991–2001.

Bethke, C. M. (1989), Modeling subsurface flow in sedimentary basins, *Geol. Rundsch.*, 78, 129–154.

Bethke, C. M. (1996), *Geochemical Reaction Modeling*, Oxford Univ. Press, New York.

Bethke, C. M., M.-K. Lee, H. A. M. Quinodoz, and W. N. Kreiling (1993), *Basin Modeling With Basin2; A Guide to Using Basin2, B2plot, B2video, and B2view*, 225 pp., Hydrogeol. Program, Univ. of Ill. at Urbana-Champaign, Urbana.

Carey, A. E., C. B. Dowling, and R. J. Poreda (2004), Alabama Gulf Coast groundwaters:  $^4\text{He}$  and  $^{14}\text{C}$  as groundwater-dating tools, *Geology*, 32, 289–292, doi:10.1130/G20081.2.

Chapelle, F. H. (2001), *Ground-Water Microbiology and Geochemistry*, John Wiley, Hoboken, N. J.

Chapelle, F. H., and L. L. Knobel (1983), Aqueous geochemistry and the exchangeable cation composition of glauconite in the Aquia Aquifer, Maryland, *Ground Water*, 21, 343–352.

Clark, I., and P. Fritz (1997), *Environmental Isotopes in Hydrogeology*, CRC Press, Boca Raton, Fla.

Cook, M. R. (1993), The Eutaw Aquifer in Alabama, *Bull. Geol. Surv. Ala.*, 156, 105 pp.

Cook, M. R. (1997), Origin and evolution of anomalous hydrogeochemical character of the Tuscaloosa aquifer system of west-central Alabama, M.S. thesis, Univ. of Ala., Tuscaloosa.

Davis, M. E. (1998), Stratigraphic and hydrogeologic framework of the Alabama coastal plain, *U.S. Geol. Surv. Water Res. Invest. Rep.*, 87-412, 1–39.

Davis, S. N., J. Fabryka-Martin, L. Wolfsberg, S. Moysey, R. Shaver, E. C. Alexander, and N. Krothe (2000), Chlorine-36 in groundwater containing low chloride concentrations, *Ground Water*, 38, 912–921.

Deming, D. (2002), *Introduction to Hydrogeology*, McGraw-Hill, New York.

Dowling, C. B., R. J. Poreda, and A. R. Basu (2003), The groundwater geochemistry of the Bengal basin: Weathering, chemisorption, and trace metal flux to the oceans, *Geochim. Cosmochim. Acta*, 67, 2117–2136.

Faure, G. (1997), *Principles of Isotope Hydrology*, John Wiley, Hoboken, N. J.

Floesser, J. A. (1996), Groundwater geochemistry of four upper Cretaceous and lower Tertiary aquifers in the Gulf Coastal Plain of southeastern Alabama, M. S. thesis, Auburn Univ., Auburn, Ala.

Fredrickson, J. K., J. M. Zachara, D. W. Kennedy, H. Dong, T. C. Onstott, N. W. Hinman, and S.-M. Li (1998), Biogenic iron mineralization accompanying the dissimilatory reduction of hydrous ferric oxide by a groundwater bacterium, *Geochim. Cosmochim. Acta*, 62, 3239–3257.

Freeze, R. A., and J. A. Cherry (1979), *Groundwater*, Prentice-Hall, Upper Saddle River, N. J.

Hendry, M. J., and F. W. Schwartz (1990), The chemical evolution of ground water in the Milk River aquifer, Canada, *Ground Water*, 28, 253–261.

Horton, J. W., Jr., I. Zietz, and T. L. Neathery (1984), Truncation of the Appalachian Piedmont beneath the Coastal Plain of Alabama: Evidence from the new magnetic data, *Geology*, 12, 51–55.

Johnson, T. M., R. C. Roback, T. L. McLing, T. D. Bullen, D. J. DePaolo, C. Doughty, R. J. Hunt, M. T. Murrell, and R. W. Smith (2000), Groundwater ‘fast paths’ in the Snake River Plain aquifer: Radiogenic isotope ratios as natural groundwater tracers, *Geology*, 28, 871–874.

King, D. T., Jr. (1990), Facies stratigraphy and relative sea-level history—Upper Cretaceous Eutaw Formation, central and eastern Alabama, *Trans. Gulf Coast Assoc. Geol. Soc.*, 40, 381–387.

Konhauser, K. O. (1998), Diversity of bacterial iron mineralization, *Earth Sci. Rev.*, 43, 91–121.

Lee, M.-K., and C. M. Bethke (1996), A model of isotopic fractionation in reacting geochemical systems, *Am. J. Sci.*, 296, 965–988.

Lee, M.-K., and J. A. Saunders (2003), Effects of pH on metals precipitation and sorption: Field bioremediation and geochemical modeling approaches, *Vadose Zone J.*, 2, 177–185.

Lee, M.-K., J. A. Saunders, R. T. Wilkin, and S. Mohammad (2005), Geochemical modeling of arsenic speciation and mobilization, in *Advances in Arsenic Research: Integration of Experimental and Observational Studies and Implications for Mitigation, Symp. Ser.*, vol. 915, edited by P. O’Day et al., pp. 398–413, Am. Chem. Soc., Washington, D. C.

Lee, R. W. (1985), Geochemistry of groundwater in Cretaceous sediments of the southeastern coastal plain of eastern Mississippi and western Alabama, *Water Resour. Res.*, 21, 1545–1556.

Lee, R. W. (1993), Geochemistry of ground water in the southeastern coastal plain aquifer system in Mississippi, Alabama, Georgia, and South Carolina, *U.S. Geol. Surv. Prof. Pap.*, 1410-D, 1–72.

- Lehmann, B. E., S. N. Davis, and J. Fabryka-Martin (1993), Atmospheric and subsurface sources of stable and radioactive nuclides used for groundwater dating, *Water Resour. Res.*, *29*, 2027–2040.
- Lehner, S. W., K. S. Savage, and J. C. Ayers (2006), Vapor growth and characterization of pyrite (FeS<sub>2</sub>) doped with Co, Ni, and As: Variations in semiconducting properties, *J. Crystal Growth*, *286*, 306–317.
- Lovley, D. R., and F. H. Chapelle (1995), Deep subsurface microbial processes, *Rev. Geophys.*, *33*, 365–381.
- Lovley, D. R., F. H. Chapelle, and E. J. P. Phillips (1990), Fe (III)-reducing bacteria in deeply buried sediments of the Atlantic coastal plain, *Geology*, *18*, 954–957.
- Lowenstam, H. A. (1981), Minerals formed by organisms, *Science*, *211*, 1126–1131.
- Mallory, M. (1993), Hydrogeology of the southeastern coastal plain aquifer system in parts of eastern Mississippi, and western Alabama, *U.S. Geol. Surv. Prof. Paper*, *1410-G*, 1–57.
- Mann, S. (1983), Mineralization in biological systems, *Struct. Bonding*, *54*, 125–174.
- Morse, J. W., and W. H. Casey (1988), Ostwald processes and mineral paragenesis in sediments, *Am. J. Sci.*, *288*, 537–560.
- Murphy, E. M., J. A. Schramke, J. K. Frederickson, H. W. Bledsoe, A. J. Francis, D. S. Sklarew, and J. C. Linehan (1992), The influence of microbial activity and sedimentary organic carbon on the isotope geochemistry of the Middendorf Aquifer, *Water Resour. Res.*, *28*, 723–740.
- Norden, S. H., and D. Sibley (1994), Dolomite stoichiometry and Ostwald's step rule, *Geochim. Cosmochim. Acta*, *58*, 191–196.
- Pal, T., P. K. Mukherjee, S. Sengupta, A. K. Bhattacharyya, and S. Shome (2002), Arsenic pollution in groundwater of West Bengal, India: An insight into the problem by subsurface sediment analysis, *Gondwana Res.*, *5*, 501–512.
- Park, J., R. A. Sanford, and C. M. Bethke (2006), Geochemical and microbiological zonation of the Middendorf Aquifer, South Carolina, *Chem. Geol.*, *230*, 88–104.
- Penny, E., M.-K. Lee, and C. Morton (2003), Groundwater and microbial processes of Alabama coastal plain aquifers, *Water Resour. Res.*, *39*(11), 1320, doi:10.1029/2003WR001963.
- Planert, M., J. S. Williams, and S. S. DeJarnette (1993), Geohydrology of the southeastern coastal plain aquifer system in Alabama, *U.S. Geol. Surv. Prof. Pap.*, *1410-H*, 1–75.
- Plummer, L. N., J. F. Busby, R. W. Lee, and B. B. Hanshaw (1990), Geochemical modeling of the Madison Aquifer in parts of Montana, Wyoming, and South Dakota, *Water Resour. Res.*, *26*, 1981–2014.
- Raymond, D. E., and C. W. Copeland (1987), Selected columnar sections for the Coastal Plain, Appalachian Plateaus, Interior Low Plateaus, and Valley and Ridge Provinces in Alabama, *Geol. Surv. Ala. Atlas Ser.*, *20*, 1–43.
- Roback, R. C., T. M. Johnson, T. L. McLing, M. T. Murrell, S. Luo, and T.-L. Ku (2001), Uranium isotopic evidence for groundwater chemical evolution and flow patterns in the eastern Snake River Plain Aquifer, Idaho, *Geol. Soc. Am. Bull.*, *113*, 1133–1141.
- Roden, E. E., and D. R. Lovley (1993), Evaluation of <sup>55</sup>Fe as a tracer of Fe (III) reduction in aquatic sediments, *Geomicrobiol. J.*, *11*, 49–56.
- Roden, E. E., M. R. Leonardo, and F. G. Ferris (2002), Immobilization of strontium during iron biomineralization coupled to dissimilatory hydrous ferric oxide reduction, *Geochim. Cosmochim. Acta*, *66*, 2823–2839.
- Romanek, C. S., C. L. Zhang, Y. Li, J. Horita, H. Vali, D. R. Cole, and T. J. Phelps (2003), Carbon and hydrogen isotope fractionations associated with dissimilatory iron-reducing bacteria, *Chem. Geol.*, *195*, 5–16.
- Saunders, J. A., and C. T. Swann (1992), Nature and origin of authigenic rhodochrosite and siderite from the Paleozoic aquifer, northeast Mississippi, U.S.A., *Appl. Geochem.*, *7*, 375–387.
- Saunders, J. A., M. A. Prichett, and R. B. Cook (1997), Geochemistry of biogenic pyrite and ferromanganese stream coatings: A bacteria connection?, *Geomicrobiol. J.*, *14*, 203–217.
- Saunders, J. A., S. Mohammad, N. E. Korte, M.-K. Lee, D. Castle, M. O. Barnett, M. Fayek, and L. Riciputi (2005), Groundwater geochemistry, microbiology and mineralogy in two arsenic-bearing Holocene alluvial aquifers from the USA, in *Advances in Arsenic Research: Integration of Experimental and Observational Studies and Implications for Mitigation, Symp. Ser.*, vol. 915, edited by P. O'Day et al., pp. 191–205, Am. Chem. Soc., Washington, D. C.
- Schwartz, F. W., and H. Zhang (2003), *Fundamentals of Ground Water*, John Wiley, Hoboken, N. J.
- Sengupta, S., P. K. Mukherjee, T. Pal, and S. Shome (2004), Nature and origin of arsenic carriers in shallow aquifer sediments of Bengal Delta, India, *Environ. Geol.*, *45*, 1071–1081.
- Small, T. D., L. A. Warren, E. E. Roden, and F. G. Ferris (1999), Sorption of strontium by bacteria, Fe (II) oxide and bacteria-Fe (III) oxide composites, *Environ. Sci. Technol.*, *33*, 4465–4470.
- Turner, J. (2006), Groundwater geochemistry, geology, and microbiology of As-contaminated groundwater in Manikganj, Bangladesh, M.S. thesis, Auburn Univ., Auburn, Ala.
- Zhang, C. L., J. Horita, D. R. Cole, J. Zhou, D. R. Lovley, and T. J. Phelps (2001), Temperature-dependent oxygen and carbon isotope fractionations of biogenic siderite, *Geochim. Cosmochim. Acta*, *65*, 2257–2271.
- Zobrist, J., P. R. Dowdle, J. A. Davis, and R. S. Oremland (2000), Mobilization of arsenite by dissimilatory reduction of adsorbed arsenate, *Environ. Sci. Technol.*, *31*, 4646–4753.

J. Griffin, M.-K. Lee, and J. Saunders, Department of Geology and Geography, Auburn University, Auburn, AL 36849, USA. (leeming@auburn.edu)

J.-S. Jean, Department of Earth Sciences, National Cheng Kung University, Tainan 701, Taiwan.

Y. Wang, Department of Geological Sciences, Florida State University, Tallahassee, FL 32306-4100, USA.